

The rotating Kinetic Energy Storage System (KESS) is suitable as temporary energy storage in electric vehicles due to its insensitivity to the number of charge-discharge cycles and its relatively high specific energy. The size and weight of the KESS for a given amount of stored energy are minimized by decreasing the moment of inertia of the rotor and increasing its speed. A small and fast rotor has the additional benefit of reducing the induced gyroscopic moments as the vehicle turns. The very high resulting rotational speed makes the magnetic bearing an essential component of the system, with the Active Magnetic Bearing (AMB) being the most common implementation. The complexity and cost of an AMB can be reduced by integration with the electric machine, resulting in a bearingless and sensorless electric machine. This review article describes the usage of magnetic bearings for FESS in vehicular applications.

Keywords: Magnetic bearing, FESS, flywheel, energy storage, electric vehicle.

## 1. Introduction

Flywheels are arguably the oldest means of storing energy, dating back to the potter's wheel in ancient Egypt. During the industrial revolution they became widely used to smooth power and convert reciprocating into rotary motion. However, the heavy, slowly moving wheels out of steel or stone bear little resemblance with the high-speed flywheels of modern day. A paradigm shift came with the realization that the energy stored in the flywheel, although proportional to its moment of inertia (weight and radius of the flywheel), increases as the square of the angular velocity,

$$E = \frac{J\omega^2}{2}, \quad (1)$$

where  $E$  is the kinetic energy of the rotor,  $J$  the moment of inertia around the principle axis of rotation and  $\omega$  the angular velocity [1]. Flywheels constructed from high-strength composite materials have lower density than steel flywheels but are ideal for storing a large amount of energy since they can cope with high rotational speeds. An additional advantage of the composite rotor is its benign failure modes [2], [3], where the rotor delaminates into long strands. This permits the use of lighter enclosures, decreasing the weight of the complete system.

The concept of the modern flywheel energy storage system, as pioneered by Post [4], consists of a composite rotor attached to an electric machine, rotating at high speed. The complete system is interfaced with the outside world by power electronics. Recent progress in the area of vehicular technology has been driven by NASA [5], and CCM, Center for Concepts in Mechatronics [6]. Flywheel technology from CCM has been used in the Avanto concept developed by Siemens as well as the *Autotram* system from the Fraunhofer

\* Corresponding author: J. Abrahamsson, Division for Electricity, Dep. of Eng. Sciences, Uppsala University, Sweden, E-mail: johan.abrahamsson@angstrom.uu.se

<sup>1</sup> Division for Electricity, Dep. of Eng. Sciences, Uppsala University, Sweden.

Gesellschaft. Benefits of the flywheel technology include: relatively high energy and power density, insensitivity to the number of charge/discharge cycles, and excellent roundtrip efficiency. Disadvantages include: relatively high stand-by losses, and complexity [7].

The high angular velocity of the flywheel required to achieve high energy density, imposes requirements on the system of which vacuum-operation and advanced bearings are the most notable ones. Bearings form an integral part of any electric machine by connecting the rotating part with the stationary. The bearings keep the rotor fixed with sufficiently high stiffness while at the same time minimizing the friction. A good bearing reduces losses, frictional heat and wear. Ball bearings has benefited greatly from recent progress in the mechanical properties of ceramics and very hard steels. The lubrication of the bearing has become the main parameter influencing lifetime. Mechanical bearings are under normal conditions the best choice for rotational speeds under 20000 rpm, whereas magnetic bearings excel at speeds over 40000 rpm [8].

The bearings inside a compact high speed FESS must handle very high rotational speeds and function in a vacuum environment which causes lubrication to evaporate and prevents convective heat transfer. These are compelling arguments for the use of magnetic bearings, which so far have found commercial success in specialized applications where traditional bearings are not applicable. Examples include high-speed centrifuges, artificial hearts and uninterruptable power supplies - applications where rolling- or sliding element bearings would produce too much friction and wear down or where the lubrication of the bearing would pollute its environment.

Magnetic bearings expose the rotor to magnetic forces in radial and axial direction in such a way that it remains levitating in stable equilibrium inside the stator even when disturbed by external forces. Due to the non-contact nature of magnetic bearings, there is no wear nor friction and no need for lubrication. Although contactless, their operation is not lossless. There may be resistive losses in the coils of electromagnets, eddy current losses and hysteresis losses. The magnitude of these losses is the principle factor limiting the storage time of kinetic energy.

## **2. Active magnetic bearings**

A charged particle located within an electrostatic field can not be confined in stable stationary equilibrium, as shown by S. Earnshaw in 1839 [9]. As a consequence, there is no static, stable magnetic configuration that levitates a permanent magnet using ferromagnetism. It can be shown that this holds true for any arrangement of permanent magnets connected mechanically to each other [10].

Actively controlled electromagnets producing a time-varying magnetic field is the most common way to circumvent the problem of instability in magnetic bearings. Displacement sensors monitor the exact position of the rotor and a control algorithm computes a voltage that when applied to the electromagnets produce a suitable magnetic field. Such a system is commonly referred to as Active Magnetic Bearing (AMB). The AMB features high stiffness, controlled damping and suppression of vibrations. The main drawbacks are complexity of the control system and cost of displacement sensors and power electronics, [11].

## 2.1. Basic concepts

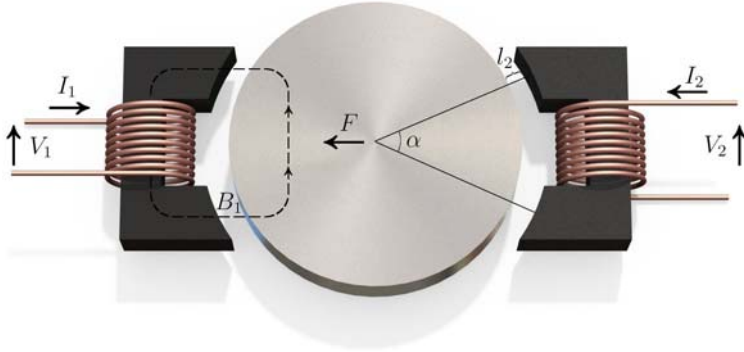


Fig. 1: Operating principle of a heteropolar electromagnetic bearing controlling one degree of freedom. A voltage,  $V$ , applied to the windings of the electromagnets drives a current,  $I$ , that generates a magnetic field,  $B$ . The intensity of the magnetic field controls the magnitude of the attractive force between actuator and rotor.

The functionality of a *heteropolar* AMB for one degree of freedom is illustrated in Fig. 1. A voltage drop over the coil drives a current, creating a magnetic flux in the air gap between electromagnet and rotor,

$$B_i = \frac{N_i \mu_0 I_i}{2l_i}, \quad (2)$$

where  $B$  is the flux density in the air gap,  $N$  the number of turns of the coil,  $\mu_0$  the permeability of free space,  $l$  the distance between the pole shoe of the electromagnet and the rotor, and the subscript  $i = 1, 2$  denotes the corresponding actuator. The total reluctance of the magnetic circuit is assumed to be located in the air gap between actuator and rotor. The resulting magnetic force acting on the rotor can be expressed as

$$F = \frac{S}{\mu_0} \cos(\alpha/2) (B_1^2 - B_2^2), \quad (3)$$

where  $S$  is the area of one stator pole and  $\alpha$  is the angle between two pole shoes. Combining equations 2 and 3 and assuming that the number of turns in the electromagnets is equal ( $N_1 = N_2 = N$ ) yields

$$F = \frac{SN^2 \mu_0}{4} \cos(\alpha/2) \left( \frac{I_1^2}{l_1^2} - \frac{I_2^2}{l_2^2} \right). \quad (4)$$

Equation 4 is highly non-linear with respect to both current and position. In order to analyze it with traditional control techniques, it must be linearized. The dependence on displacement may be linearized by choosing an operating point,  $l$ , and only allowing small displacements,  $x$ , around it. The dependence on current may be linearized by introducing a constant *bias current*,  $I_b$ , and a regulating current,  $I_r$ . The current flowing through electromagnet 1 is set to  $I_b + I_r$  and through electromagnet 2 to  $I_b - I_r$ .  $I_b$  is normally set to 50% of the rated current of the electromagnet. The linearized force equation becomes

$$F \approx \frac{SN^2\mu_0 I_b^2}{l^2} \cos(\alpha/2) \left( \frac{I_r}{I_b} + \frac{x}{l} \right). \quad (5)$$

The force is now a linear function of current and position. The drawback is the additional power loss associated with the bias current. For a more detailed introduction to the function of the active magnetic bearing, see [11] and [12].

## 2.2. Losses

The losses in an AMB are mainly due to resistive heating in the coils of the electromagnets and eddy-currents in the core and target material [12]. A large part of these losses are due to the bias current for linearization, which can not be removed completely, since this not only would destroy linearity, but additionally create a singularity in the control [13]. Much effort has in recent years been put into finding ways of reducing this current without compromising bearing stability, while minimizing controller complexity.

A reduction of power of up to 75% was reported in [14] where a variable bias current was introduced, which was continuously adjusted depending on the dynamic requirements. In [15] a similar approach was pursued, resulting in increased stability and a decrease of power loss as compared to the linear case. Several non-linear controls were investigated in [16], where losses were decreased by 80% compared to the linear case at the expense of a more complicated controller.

A hardware solution for the optimization of losses was presented in [17], where the bias current was generated not from electromagnets, but from permanent magnets with a separate flux path. This approach did not have a large impact on the eddy current loss, but the resistive loss associated with the bias current was eliminated, reducing the total loss of the bearing by 50%.

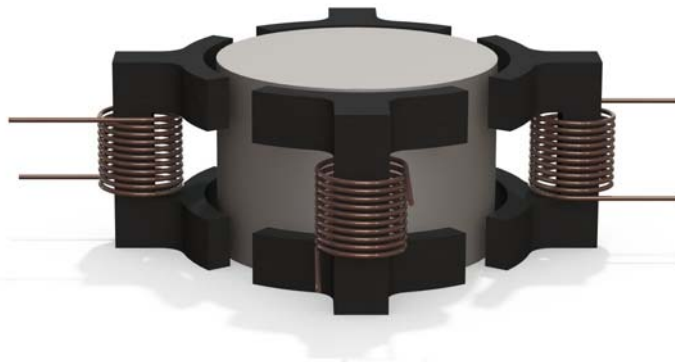


Fig. 2: Schematic view of a homopolar electromagnetic bearing controlling two degrees of freedom. As a surface element on the rotor passes from one actuator to the next, it experiences a change of intensity of the magnetic field, but not a change of sign as in the heteropolar case. This reduces loss due to eddy-currents.

A *homopolar* bearing design reduces losses due to eddy currents, see Fig. 2. As a section of the rotor passes from one pole shoe to the next, it experiences a smaller change of flux as

compared with the heteropolar case. This effect was investigated in [18], where it was shown that the power loss in the homopolar set-up is significantly lower than that of the heteropolar configuration.

Three actuators instead of four may be used, to further reduce losses. This additionally reduces the number of power amplifiers needed in the system, as well as the number of parts, at the cost of strong non-linearities from the flux-coupling between the actuators. A control strategy based on local PD algorithm was presented in [19]. An optimized three-pole AMB only employing two power amplifiers was suggested in [20] and experimentally verified in [21].

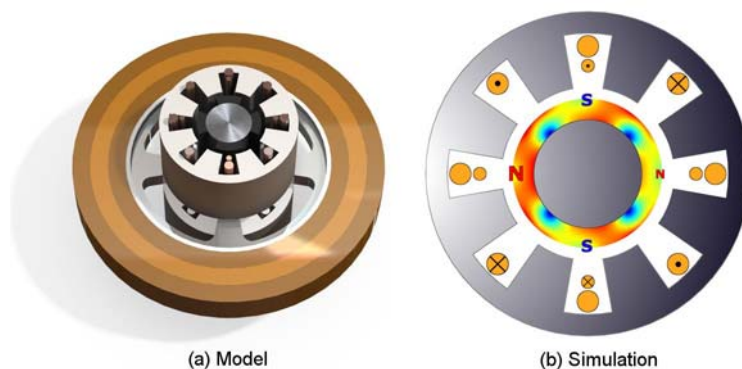


Fig. 3: Model of a two-phase bearingless machine. a) The stator consists of a thicker four-pole motor winding and a thinner two-pole suspension winding. It is split into two separate units, one above the rotor, and one below. b) Simulation of the resulting magnetic field. The motor winding generates a four-pole magnetic field, creating a torque. The suspension winding increases the intensity of the magnetic field on the left side and decreases it on the right side, creating a force in horizontal direction.

### 2.3. Bearingless drive

Large savings in complexity and cost can be achieved by integrating the active magnetic bearing with the electric machine and its controller. One example of this is the concept of the bearingless drive [11]. Here, the actuators of the AMB are integrated into the stator windings of the electric machine, see Fig. 3. This not only reduces the cost of the bearing but also the complexity and additional number of parts needed to suspend the rotor since the existing stator windings and controller of the electric machine can be used.

A double wound stator split into two separate units can be used to achieve four-axis suspension. The secondary winding creates a magnetic field that, when superposed on the magnetic field from the primary winding, generates a radial force on the rotor. An example can be found in [22] where a bearingless drive with coreless stator was suggested as temporary energy storage for various types of systems for generation of renewable energy, including wave, wind and tidal energy.

Although the bearingless drive is especially attractive to systems that already employ a double winding concept, [23] [24], it is also possible to implement the bearingless

functionality in an electric machine with a single winding. Six separate phases are then required [25].

#### 2.4. Sensorless operation

Another important field of integration lies in sensorless operation where the actuators of the AMB are used not only for force generation but also to deduce the instantaneous length of the air-gap between rotor and stator by measurement of voltage and current through the coils of the electromagnets.

One way of achieving this was demonstrated in [26] where self sensing was combined with zero-bias-current control. A resonance circuit transmitted the PWM carrier signal to the electromagnetic actuators. Their response to this signal was measured and the air-gap calculated. The test set-up (a turbomolecular pump) operated stably up until its rated speed of 45000 rpm.

The displacement sensors usually constitute a large part of the cost of magnetic bearings, so self-sensing techniques can potentially decrease the total cost and complexity of the system drastically. Recent work includes efforts to improve robustness of the resulting system [27]. For an excellent overview of the current status in this field see [28].

### 3. Hybrid and passive magnetic bearings

Progress over the last decade has produced rare-earth permanent magnets (e.g. the neodymium magnet) with magnetic field in excess of 1.4 T allowing compact permanent magnets to produce high forces. This has spawned renewed interest in combining passive elements with the AMB, creating a Hybrid Magnetic Bearing (HMB).

In a five-axis AMB the electromagnets must not only maintain the position of the rotor, but also support the complete weight of the levitated object. This introduces a bias-current in the electromagnet located in the direction of gravity which creates resistive losses and heating. Permanent magnets can be used for this task, either in repulsive or attractive mode [29].

In the special case of a vertical axis flywheel with permanent magnets in repulsive mode, the following equation holds [30],

$$K_a + 2K_r \leq 0, \quad (6)$$

where  $K_a$  is the stiffness in axial direction and  $K_r$  the stiffness in radial direction. This means that although the axial stiffness (created by the repulsive permanent magnets and gravity) is greater than zero, the bearing will have negative stiffness in radial direction. This increased instability must be dealt with by radial AMB:s.

A functioning five-axis Passive Magnetic Bearing (PMB) may be constructed in spite of Earnshaws theorem due to the rotary motion of the levitated object. This motion can be used either to generate a varying magnetic field in an external closed loop [30] or, as in the case of the Levitron<sup>TM</sup>, for gyroscopic stabilization of the rotating top [31]. In [32] a passive linear maglev system was proposed. Stabilizing forces were generated through induced eddy-currents from the interaction between permanent magnets attached to the vehicle and stationary aluminum rails. Pure PMB:s have generally very low losses and do

not need an active controller. The drawbacks are low stiffness, low damping and limited regions of stability.

#### 4. Rotor design

The material properties of the rotor determine the maximum amount of energy that can be stored in a FESS. At a certain velocity the internal stress causes the rotor to crack, leading to rapid desintegration. The highest possible energy density of a composite flywheel is achieved in a thin rim [1], where the radial stresses are very small and the critical factor is the hoop stress. The energy density,  $Q$ , ignoring the weight of the hub, becomes

$$Q = \frac{\sigma}{2\rho}, \quad (7)$$

where  $\sigma$  is the strength and  $\rho$  the density of the material.

There are two main problems when designing a rotor in the shape of a thin rim. Firstly, the low energy density by volume caused by the empty space within the rim leads to a system with low specific energy since the vacuum enclosure that constitutes a large part of the weight of the system becomes big. Secondly, the rim is connected to a hub that must be able to withstand almost as high rotational velocity as the rim.

A thicker rim could solve both of these problems. However, the radial stress increases with increasing thickness due to the differences in radial growth over the rim. A circumferentially wound unidirectional composite material has typically less than 1/50 the strength in radial direction compared to circumferential direction. Too high radial stress causes the rotor to fail by delamination, creating an inverse relation between the specific energy and energy density by volume of the rotor.

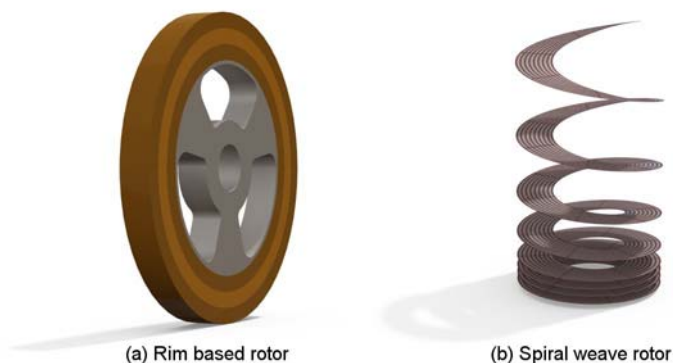


Fig. 4: Two approaches for optimization of total strength of rotors made of composite material. a) The radial forces are reduced by constructing the rim from high-strength composite rings separated by elastic material. b) The radial strength of the composite is increased by using a spiral weave composite at the expense of decreased hoop strength.

Different approaches have been followed in order to optimize the total strength of composite rotors. The radial stress may be reduced by winding high-strength carbon fibers glued together with epoxy resin in the circumferential direction, creating several separate concentric rings. The rings are then either press-fitted with a radial preload, or separated by

layers of material with a lower Young's modulus, see Fig. 4a. The radial strength of the composite material may be increased by creating a bi-directional spiral-shaped composite weave at the expense of reduced strength in circumferential direction, see Fig. 4b and [33].

The first of these approaches was implemented in [34] where a rim with a combination of high-strength graphite fiber (T700-12K, Toray) and flexible E-Glass fiber (RS2300-366) was used. A rotor with 2 rims, storing 0.5 kWh, was simulated and built, achieving a maximum specific energy of 64.8 Wh/kg, and an energy density of 89 Wh/L. Simulations showed that a rotor built with 4 rims storing 0.5 kWh would achieve a maximum specific energy of 81 Wh/kg and an energy density of 115 Wh/L.

A similar approach was used in [35], where a specific energy of 195 Wh/kg was achieved by accelerating a rim of composite material to a peripheral speed of 1310 m/s. The rim was made of 4 concentric press fitted rings of Toray T1000 and epoxy. The hub was made of high-strength aluminum alloy (7075), which was cooled by liquid nitrogen before fitted into the rim. The energy density over the swept volume was 112 Wh/L, and the high-strength aluminum alloy used in the spoked hub of the rotor was stressed beyond its limit of plastic deformation already at a rim speed of 1100 m/s (corresponding to 70% of the maximum energy content).

## 5. Energy density

The system described in [23] can be assumed to require a flywheel capable of storing 0.5 kWh. The size of the corresponding enclosure can, very roughly, be found by further assuming a composite rotor with a specific energy of 50 Wh/kg and energy density of 50 Wh/L. The enclosure should be able to house 10 L and 10 kg of rotating mass. The minimum surface area,  $A$ , for a cylinder with given volume,  $V$ , can be found from

$$\begin{aligned} A &= 2\pi r^2 + 2\pi r h \\ V &= \pi r^2 h, \end{aligned} \tag{8}$$

where  $r$  is the radius of the base plate and  $h$  the height of the cylinder. Combining these two equations yields that the surface area is minimized when  $h = 2r$ . An enclosure of 10 L would therefore have a radius of 0.12 m.

The wall thickness of vacuum chamber made from steel with a density,  $\rho$ , of 7850 kg/m<sup>3</sup> is, as a rule of thumb, 1% of the diameter of the chamber [1]. The weight,  $W$ , of the enclosure becomes

$$W = 0.02\rho r(2\pi r^2 + 2\pi r h), \tag{9}$$

which when evaluated becomes approximately 5 kg, resulting in a specific energy of rotor and enclosure of 33 Wh/kg.

The weights of the electric machine, associated power electronics and control system need to be estimated in order to calculate a realistic total energy density. However, they depend to a very large extent on the required power capabilities of the system. A specific energy of the complete system between 15 Wh/kg and 25 Wh/kg is reasonable, as a very rough estimate. The corresponding specific power could reach values of over 1000 W/kg, see [4].

## 6. Comparison of complete systems

It is difficult to make a general and fair comparison of different means of storing energy since their properties depend to a large extent on requirements and design. The specific energy of batteries depends on the power output since energy is lost over internal resistance. The specific power is in turn related to the cycle life. A standardized comparison can be achieved by evaluating the specific power corresponding to an efficiency of 95%. This guarantees a long cycle life, but it should be remembered that the battery is able to output bursts of power up to five times higher for short periods of time.

The power output of the FESS depends only weakly on the weight of the rotor. It depends on the design of the electric machine and the power electronics. The specific energy and energy density by volume is to a large degree also dependent on peripheral components, especially type and size of the enclosure. The total weight and volume of these components is typically higher than the weight of the rotor, especially if the system requires suspension in gimbals.

Table 1: Comparison of energy storage systems

| Type of energy storage           | Specific energy [Wh/kg] | Specific power [W/kg] |
|----------------------------------|-------------------------|-----------------------|
| EV batt. (Li-ion)                | 140                     | 90                    |
| HEV batt. (Li-ion)               | 77                      | 256                   |
| Ultracapacitor                   | 4                       | 513                   |
| Flywheel (steel)                 | 3                       | 280                   |
| Flywheel (composite) (estimated) | 15-25                   | >1000                 |

Table 1 contains a comparison the most common properties of a number of specific complete energy storage systems currently considered for electric vehicles. The batteries are produced by Saft [36], the ultracapacitor by Maxwell Technologies [37] and the steel flywheel have been designed by the university of Texas for usage as temporary energy storage in a bus [38]. The flywheel system includes housing and gimbals. Noticeable is the difference in energy density between batteries optimized for Hybrid Electric Vehicles (HEV) with high power capabilities, and batteries optimized for Electric Vehicles (EV) with high energy density.

The energy densities listed refers to the total stored energy in the systems. The usable energy is often significantly lower. Deep-cycling of battery systems are often avoided in order to prolong cycle life. This reduces the usable energy by 25%- 50%. Flywheel systems are often operated down to half of the maximum rated speed, reducing the usable energy by 25%.

## 7. Gyroscopic moment

Kinetic energy storage systems located in non-stationary applications experience gyroscopic moments associated with roll, pitch or yaw moments of the vehicle [1]. The gyroscopic moment can be calculated by

$$\overline{M} = J\overline{\omega} \times \overline{\Omega}, \quad (10)$$

where  $\overline{M}$  is the gyroscopic moment generated by  $\overline{\Omega}$ , the angular velocity of the FESS. The rotational axis of the flywheel should therefore be positioned vertically since the highest angular velocities during normal driving occur when turning.

Combining equations 1 and 10, and assuming a vertically aligned flywheel exposed to a pure roll or pitch motion yields

$$M = \frac{2E\Omega}{\omega}. \quad (11)$$

This means that the magnitude of the gyroscopic moment decreases linearly with increasing rotational speed (and thereby decreasing moment of inertia) for a certain amount of stored energy.

Using the guideline from the Swedish road administration regarding the allowable change of inclination of roads for vehicles, [39], the worst case is  $\Omega = 0.035$  rad/s (vehicle moving with 50 km/h on a road with a vertical radius of 400 m). A slowly moving steel flywheel with  $\omega = 630$  rad/s, storing  $E = 1$  kWh would experience a gyroscopic moment of 400 Nm. A high-speed composite flywheel storing the same amount of energy, but rotating with  $\omega = 6300$  rad/s would in comparison only experience 40 Nm.

The magnetic bearings could be designed to cope with the gyroscopic moments associated with the roll and pitch of the vehicle during normal driving, possibly using touchdown bearings for extreme situations. A gyroscopic suspension could alternatively be constructed around the flywheel, at the expense of increased complexity and lower specific energy. An intelligent gyroscopic suspension was developed in [40] where a system of motor controlled gimbals was used to minimize forces on the bearings.

## 8. Conclusion

Modern flywheel energy storage systems fill a unique niche between ultracapacitors with low energy density and high power output on one hand and modern lithium batteries with high energy density but limited power capabilities on the other. Their very long cycle life and high power capabilities make them ideal for applications where a relatively large amount of energy needs to be stored and accessed frequently.

Kinetic energy storage systems used in moving applications experience gyroscopic moments that may be eliminated by suspending the complete FESS in a system of gimbals. This increases the complexity of the system and decreases the energy density. The magnetic bearings could, in some cases, be designed to cope with the resulting moments, especially for flywheels storing a relatively low amount of energy while spinning at high angular speed. The induced gyroscopic moment decreases linearly with increasing rotational velocity of the flywheel for a given amount of stored energy.

It has been suggested that the FESS could be used as main energy storage in electric vehicles [4]. The benefits would be long cycle life and high power density, allowing rapid refueling and high driving torque. The practical applicability of this idea is presently limited by the specific energy and stand-by losses of the FESS. The stand-by losses may be reduced significantly by decreasing the bias current of the magnetic bearings, either by introducing a non-linear control or by using permanent magnets, and by employing a homopolar set-up of the magnetic actuators. Purely passive magnetic bearings could be used to achieve the very low losses needed for long term energy storage, i.e. when the

vehicle is parked, but must be combined with active magnetic bearings in order to handle the dynamic forces when the vehicle is moving.

The case for the FESS as peak energy buffer is presently stronger due to its capability to reliably transfer a large amount of energy quickly and with high round-trip efficiency without degradation of performance over time [41], [42], [43]. The relatively high energy density of the FESS makes it competitive when compared with ultracapacitors. This technology would enable efficient regenerative braking and usage of a primary energy source optimized for energy density. Here, the main issue is the reduction of cost and complexity. The magnetic bearings should be robust (have few parts), compact and cheap. One way of achieving this would be a system with a double wound bearingless electric machine working in sensorless operation. The system should be small and fast enough that the gyroscopic moments can be handled by the bearings and no gimbals are needed for suspension.

## References

- [1] G. Genta, *Kinetic Energy Storage: Theory and Practice of Advanced Flywheel Systems*, Butterworth-Heinemann Ltd, London, 1985.
- [2] G. Genta, Spin tests on medium energy density flywheels, *Composites*, vol. 13(1), 1982, 38-46.
- [3] R. Thompson, J. Kramer, and R. Hayes, Response of an urban bus flywheel battery to a rapid loss-of-vacuum event, *Journal of Advanced Materials*, 37(3), 2005, 42-50.
- [4] R. Post, T. Fowler, and S. Post, A high-efficiency electromechanical battery, *Proceedings of the IEEE*, 81(3), 1993, 462-474.
- [5] B. Alexander, R. Rarick, and Lili Dong, A novel application of an extended state observer for high performance control of NASAs HSS Flywheel and fault detection, *American Control Conference*, 2008, 5216-5221.
- [6] B. Siuru, Testing many technologies: Fraunhofer's Auto Tram people mover includes hybrid, fuel cell versions, *Diesel Progress North American Edition*, 2007.
- [7] I. Vajda, Z. Kohari, L. Benko, V. Meerovich, and W. Gawalek, LARGE SCALE - Superconducting Rotating Machinery and Levitation – Maglev - Investigation of Joint Operation of a Superconducting Kinetic Energy Storage (Flywheel) and Solar Cells, *IEEE transactions on applied superconductivity*, 13(2), 2003, 2169.
- [8] H. Liu, Flywheel energy storage—An upswing technology for energy sustainability, *Energy and buildings*, 39(5), 2007, 599.
- [9] R. Bassani, Earnshaw (1805-1888) and Passive Magnetic Levitation, *Meccanica Milano*, 41(4), 2006, 375-389.
- [10] R.P. Feynman, R.B. Leighton, and M. Sands, *The Feynman Lectures on Physics including Feynman's Tips on Physics: The Definitive and Extended Edition*, Addison Wesley, Munchen, 2005.
- [11] A. Chiba, T. Fukao, O. Ichikawa, M. Oshima, M. Takemoto, and D.G. Dorrell, *Magnetic Bearings and Bearingless Drives*, Newnes, London, 2005.
- [12] B. Wilson, Control designs for low-loss active magnetic bearing theory and implementation, Ph.D. thesis, Georgia Institute of Technology, Georgia, USA, 2004.
- [13] P. Tsiotras and B. Wilson, Zero- and low-bias control designs for active magnetic bearings, *IEEE Transactions on Control Systems Technology*, 11(6), 2003, 889-904.
- [14] M. Necip Sahinkaya and Ahu E. Hartavi, Variable Bias Current in Magnetic Bearings for Energy Optimization, *IEEE Transactions on Magnetics*, 43(3), 2007, 1052-1060.
- [15] M. de Queiroz and Pradhananga, Control of Magnetic Levitation Systems With Reduced Steady-State Power Losses, *IEEE Transactions on Control Systems Technology*, 15(6), 2007, 1096-1102.
- [16] A. Charara, J. De Miras, and B. Caron, Nonlinear control of a magnetic levitation system without premagnetization, *IEEE Transactions on Control Systems Technology*, 4(5), 1996, 513-523.
- [17] X. Yanliang, D. Yueqin, W. Xiuhe, and K. Yu, Analysis of hybrid magnetic bearing with a permanent magnet in the rotor by FEM, *IEEE Transactions on Magnetics*, 42(4), 2006, 1363-1366.
- [18] H.Y. Kim and C.W. Lee, Analysis of Eddy-Current Loss for Design of Small Active Magnetic Bearings With Solid Core and Rotor, *IEEE transactions on Magnetics*, 40(5), 2004, 3293.
- [19] A. Pilat, PD control strategy for 3 coils AMB, *Tenth International Symposium on Magnetic Bearings*, 2006, 34-39.
- [20] S.L. Chen and C.T. Hsu, Optimal design of a three-pole active magnetic bearing, *IEEE Transactions on Magnetics*, 38(5), 2002, 3458-3466.

- [21] S.L. Chen, S.H. Chen, and S.T. Yan, Experimental validation of a current-controlled three-pole magnetic rotor-bearing system, *IEEE Transactions on Magnetics*, 41(1), 2005, 99-112.
- [22] M. Ooshima, Design and Analyses of a Coreless-Stator-Type Bearingless Motor Generator for Clean Energy Generation and Storage Systems, *IEEE Transactions on Magnetics*, 42(10), 2006, 3461-3463.
- [23] J. Santiago, J. Oliveira, J. Lundin, J. Abrahamsson, A. Larsson, and H. Bernhoff, Design Parameters Calculation of a Novel Driveline for Electric Vehicles, *World Electric Vehicle Journal*, 2009, Vol. 3.
- [24] M. Leijon, H. Bernhoff, and B. Bolund, System for storage of power, *Patent WO/2004/045884*, 2004.
- [25] M. Kang, J. Huang, J.Q. Yang, and H.B. Jiang, Analysis and experiment of a 6-phase bearingless induction motor, *International Conference on Electrical Machines and Systems*, 2008, 990-994.
- [26] Y. Kato, T. Yoshida, and K. Ohniwa, Self-sensing active magnetic bearings with zero-bias-current control, *Electrical Engineering in Japan*, 165(2), 2008, 69-76.
- [27] K. Peterson, R. Middleton, and J. Freudenberg, Fundamental limitations in self sensing magnetic bearings when modeled as linear periodic systems, *American Control Conference*, 2006, 6.
- [28] E.H. Maslen, Selfsensing for active magnetic bearings: overview and status, *Tenth International Symposium on Magnetic Bearings*, Martigny Switzerland, 2006, 10-15.
- [29] D.F. Wilcock and M. Eusepi, A Passive Magnetic-Thrust Bearing for Energy-Storage Flywheels, *Tribology Transactions*, 25(1), 1982, 7.
- [30] A. Filatov and E. Maslen, Passive magnetic bearing for flywheel energy storage systems, *IEEE Transactions on Magnetics*, 37(6), 2001, 3913-3924.
- [31] G. Genta, C. Delprete, and D. Rondano, Gyroscopic Stabilization of Passive Magnetic Levitation, *Meccanica*, 34(6), 1999, 411-424.
- [32] A. Musolino, R. Rizzo, M. Tucci, and V. Matrosov, A New Passive Maglev System Based on Eddy Current Stabilization, *IEEE Transactions on Magnetics*, 45(3), 2009, 984-987.
- [33] D. Maass and D.M. Hoon, Spiral woven composite flywheel rim, *Patent US6029350*, 1998.
- [34] S.K. Ha, J.H. Kim, and Y.H. Han, Design of a Hybrid Composite Flywheel Multi-rim Rotor System using Geometric Scaling Factors, *Journal of Composite Materials*, 42(8), 2008, 771-785.
- [35] K. Takahashi, S. Kitade, and H. Morita, Development of high speed composite flywheel rotors for energy storage systems, *Advanced Composite Materials*, 11, 2002, 40-49.
- [36] A. Burke, Batteries and Ultracapacitors for Electric, Hybrid, and Fuel Cell Vehicles, *Proceedings of the IEEE*, 95(4), 2007, 806-820.
- [37] Maxwell Technologies, *BMOD0165 P048*.
- [38] C. Hearn, M. Flynn, M. Lewis, R. Thompson, B. Murphy, and R. Longoria, Low Cost Flywheel Energy Storage for a Fuel Cell Powered Transit Bus, *IEEE Vehicle Power and Propulsion Conference*, 2007, 829-836.
- [39] The Swedish Road Administration, Vägar och gators utformning, *ISSN 1401-9612*, 2004.
- [40] H. Nakai, A. Matsuda, and M. Suzuki, Development and testing of the suspension system for a flywheel battery, *Control Engineering Practice*, 9(), 2001, 1039-1046.
- [41] A. Ruddell, ENK5-CT-2000-20336 Storage Technology Report: WP-ST6 Flywheel, *Investigations on Storage Technologies for Intermittent Renewable Energies*, 2003.
- [42] R. Hebner, J. Beno, and A.Walls, Flywheel batteries come around again, *IEEE Spectrum*, 39(4), 2002, 46-51.
- [43] B. Bolund, H. Bernhoff and M. Leijon, Flywheel energy and power storage systems, *Renewable and Sustainable Energy Reviews*, 11(2), 235-258, 2007.